Hindawi
Mathematical Problems in Engineering
Volume 2020, Article ID 9706183, 18 pages
https://doi.org/10.1155/2020/9706183

Research Article

Numerical Investigation of the Rock Cutting Performance of a Circular Sawblade

Zhiwen Wang[1], **Qingliang Zeng**[1], **Zhenguo Lu**[2], **Zhihai Liu**[2] and **Xu Li**[1]

[1]*College of Mechanical and Electronic Engineering, Shandong University of Science and Technology, Qingdao 266590, China*
[2]*College of Transportation, Shandong University of Science and Technology, Qingdao 266590, China*

Correspondence should be addressed to Qingliang Zeng; qlzeng@sdust.edu.cn

Received 28 April 2020; Revised 20 August 2020; Accepted 14 September 2020; Published 25 September 2020

Academic Editor: Haipeng Peng

Copyright © 2020 Zhiwen Wang et al. This is an open access article distributed under the Creative Commons Attribution License, which permits unrestricted use, distribution, and reproduction in any medium, provided the original work is properly cited.

The rock cutting process with a circular sawblade and the rock breaking mechanism of rock are studied with a numerical simulation method in this paper. The influence of cutting parameters of the circular sawblade on cutting force, rock damage, and specific cutting energy in the process of circular sawblade cutting rock is researched. The cutting force increases with the feed speed and an increase in cutting depth and decline in rotation speed. Cutting rock with double circular sawblades can reduce cutting force. However, the specific cutting energy declines with the increase in cutting depth and the decline in the distance between the double circular sawblades. Cutting parameters have a great influence on the damage range of rock. The research results can be applied to rock processing with a circular sawblade.

1. Introduction

Natural stone is an important building material, and the circular sawblade is widely applied in natural stone processing. The influences of circular sawblade cutting parameters on the cutting performance are studied. Many experts and scholars at home and abroad have penetrated into research on cutting rock with a sawblade.

The brittleness of the rock makes rock processing very difficult. Diamond sawblade is the best choice in rock processing. Therefore, many scholars have investigated cutting rock with a sawblade. Zhang et al. explored the wear performance of diamond tools with different sawing trajectories in stone processing with experiments [1]. Yan et al. established the mathematical model to research the influence of a diamond-coated tool on cutting characteristics in machining of natural marble [2]. Oh et al. researched the effect of the abrasive feed rate and the particle size distribution on the rock cutting performance [3]. Wang et al. investigated the effect of the cutting parameters and abrasive angle on a rock fragment and cutting forces and demonstrated the feasibility and reliability of FDEM in simulating rock machining [4]. Dong et al. applied the scanning electron microscopy and the 3D laser microscope in sawing experiments to study the wear characteristics of diamond tools during cutting granite [5]. Jerro et al. built the theoretical chip morphology and the relationship between the force and cutting parameters [6]. Turchetta et al. expressed the influence of pretwisting and tensioning of wire on the cutting force and optimized [7]. Zhong et al. discussed the influence of fluid and the shale rock interaction on rock [8]. Karakurt et al. expressed the influence of cutting parameters and the petrophysical parameters on cutting force [9]. Buyuksagis and Goktan conducted experiments of a circular sawblade cutting seven types of marble to investigate the influence of cutting parameters on specific cutting energy [10]. Ersoy and Atici researched the influence of operation and rock parameters on the performance of saw with experiments [11]. Fener et al. studied the rock cutting process with a circular diamond sawblade to predict the performance of cutting carbonate rocks [12]. Tumac investigated the rock parameters of Turkish carbonate rock cutting with a large diameter circular saw to predict the cutting performance [13]. Wang et al. performed single cutting experiments to research the influence of milling parameters on marble fragments and cutting force [14].

Kahraman et al. predicted the sawability of carbonated rock with the artificial network from shear strength parameters [15]. Tumac researched the cutting performance of a circular sawblade with the artificial neural network and geological origin of the rock [16, 17]. Wie et al., based on a new method of fuzzy mathematics, established the relationship between the sawability and the mechanical properties of granite [18]. Kahraman et al. carried out experiments of cutting rock with large diameter diamond saws and analyzed with multiple curvilinear regression analysis to build the predicting model of sawability of carbonate rock [19]; besides, they researched the relationship between sawability and undertaken hardness [20]. According to operation and rock parameters, Yurdakul and Akdas established the predicting model using statistical methods to predict the specific cutting energy [21]. Güney established the performance prediction model of a larger diameter saw based on rock parameters [22].

Many scholars have researched the influence of operation and rock parameters on the diamond saws cutting performance and specific cutting energy with experimental and theoretical methods. However, few research studies are based on the method of numerical simulation to investigate the damage of rock with a circular sawblade cutting rock. Therefore, this paper establishes the numerical simulation models to research the influence of various parameters on the cutting performance of a circular sawblade, with feed speeds of 0.10, 0.15, 0.20, 0.25, and 0.30 m/min and rotation speeds of 1000, 1500, 2000, 2500, and 3000 r/min, the cutting depths set as 10, 20, 30, 40, 50, and 60 mm, and the distance of double diamond sawblades set as 10, 20, 30, 40, and 50 mm.

2. The Cutting Force Components Demonstration

The rotation speed direction of a circular sawblade has a great effect on the cutting performance. It is defined that the feed speed and the rotation speed in the same direction is the forward cutting while the opposite direction is the reverse cutting. There are two kinds of cutting force models of circular sawblade cutting rock with two directions of rotation speed, as is shown in Figure 1. The cutting thickness of the forward cutting is from thin to thick. When circular sawblade contacts the rock which immediately cuts the rock, the circular sawblade will slide on the rock surface and the cutting thickness increases slowly, which is advantageous to cutting rock. However, the cutting thickness of the circular sawblade reverse cutting is from thick to thin, and the circular sawblade cuts rock from the uncutting surface to the cutting surface. In addition, the reverse cutting is starting from the uncutting surface into the surface of the hard layer, and the circular sawblade is subject to a great impact load. The cutting thickness and the contact time of the forward cutting and reverse cutting are different, and the damage of rock is different in the process of a circular sawblade cutting rock. According to experience, the cutting performance of the circular sawblade with forward cutting is obviously higher than that of the reverse cutting. When the circular sawblade cuts hard rock, the forward cutting is more suitable to the rock cutting.

The tangential force and normal force are the main components of cutting force in a circular sawblade cutting rock. However, the axial force is much smaller than tangential force and normal force. The axial force is neglected during a circular saw cutting rock in the calculation for formulas. The cutting force can be obtained by the equation as follows:

$$F_c = \sqrt{F_v^2 + F_h^2}, \tag{1}$$

where F_c is the cutting force, F_v is the vertical force, and F_h is the horizontal force.

The contact angle θ between the circular sawblade and rock is shown as follows:

$$\theta = \cos^{-1}\left(1 - \frac{2l_p}{d}\right), \tag{2}$$

where l_p is the cutting depth and d is the diameter of the circular sawblade.

The angle μ between the cutting force and the vertical force is as follows:

$$\mu = \cos^{-1}\left(\frac{F_v}{F_c}\right). \tag{3}$$

The tangential force F_t and the normal force F_n are the components of the cutting force F_c.

$$\begin{aligned} F_t &= F_c \sin\gamma, \\ F_n &= F_c \cos\gamma, \end{aligned} \tag{4}$$

where

$$\begin{aligned} \gamma &= |\mu - A\theta|, \\ A &= \frac{\gamma \pm \mu}{\theta}. \end{aligned} \tag{5}$$

The value of A depends on the location of the circular sawblade with rock. The application point of the cutting force on the arc θ of the contact between the sawblade and the rock decides the value of A. However, the cutting depth and the length of the contact between the circular sawblade and rock are small, which makes A difficult to obtain. For the slow cutting, $A = 0.67$ is consistent with the distribution of triangular force intensity along the grinding zone [23, 24].

3. Establishing a Numerical Simulation Model

3.1. Geometric Model and Boundaries. In order to research the rock damage and the circular sawblade cutting performance, the geometric model of a circular sawblade cutting rock is established with Solidworks software, and then, the geometric model is imported to the ANSYS/LS-DYNA software to establish the circular sawblade cutting rock numerical simulation model.

The diameter of the circular sawblade is 380 mm, and it has 24 segments with the length of 40 mm, height of 15 mm,

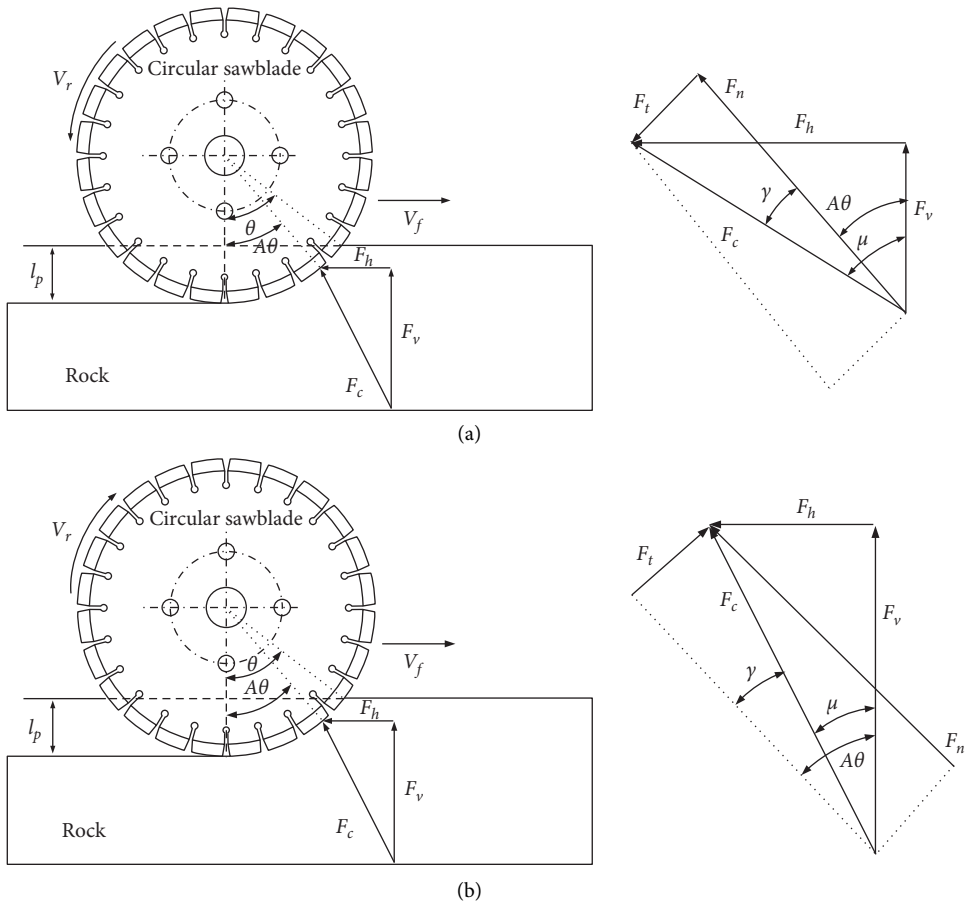

Figure 1: Force model of a circular sawblade cutting rock: (a) The force model of a circular sawblade cutting rock with forward cutting; (b) the force model of a circular sawblade cutting rock with reverse cutting.

and thickness of 3.4 mm. The rock is a cuboid which is 500 mm in length, 150 mm in width, and 125 mm in height. The hexahedral element SOLID164 is used to mesh the circular sawblade and the rock, and the smallest size of rock element is 1 mm. The model is meshed by local mesh refinement that can reduce the number of grids to improve calculation speed, as well as to ensure the computation accuracy. The key parameters of rock material are plotted in Table 1.

Constrains are applied to the numerical simulation model. The full constraints are applied to the bottom surface, the displacements constraints in the X- and Y-direction are applied to right and left surfaces, and the displacements constraints in the Y- and Z-direction are applied to the front and back surfaces. The displacements constraints in the X- and Y-direction and the rotation constraints around the Y- and Z-axis are added to the circular sawblade, as shown in Figure 2. By adding the nonboundary reflection condition to the noncutting surface of the rock, the small rock model can be used to simulate the large rock. The contact types between the circular sawblade and rock are defined as the ERODING_SURFACE_AND_SURFACE and AUTOMATIC_GENERAL. The simulation time is set as 5 minutes, and a d3plot file is exported with each step lasting 1 s. The solver in LS-DYNA/ANSYS has no limits for CPU cores, and the circular sawblade cutting rock simulation model is efficiently performed on the workstation for 45 hours.

3.2. The RHT Constitutive Model. The RHT model is divided into three stages: the elastic stage, linear strengthening stage, and damage softening stage. The standardized pressure expression is $p^* = (p/f_c)$, where f_c is the uniaxial compressive stress. The equivalent stress intensity expression for the failure surface is

$$\sigma_{\text{fail}}(p, \theta, \dot{\varepsilon}) = f_c \cdot \sigma^*_{\text{TXC}}(p_s) \cdot R_3(\theta) \cdot F_{\text{rate}}(\dot{\varepsilon}), \quad (6)$$

where $\sigma^*_{\text{TXC}}(p_s)$ is the equivalent stress intensity of the compressive meridian of the quasistatic failure surface equation, $R_3(\theta)$ is the load angle factor, $p_s = (p/(F_{\text{rate}}(\dot{\varepsilon})))$ is the quasistatic pressured, and $F_{\text{rate}}(\dot{\varepsilon})$ is the compressive strain rate dynamic increase factor, with the expression as follows:

Table 1: The related parameters of rock material [25].

Parameters	Mass density (kg/m^3)	Young's modulus (GPa)	Uniaxial compressive strength (MPa)	Brazilian tensile strength (MPa)
Value	2.7e3	45.5	120.7	12.1

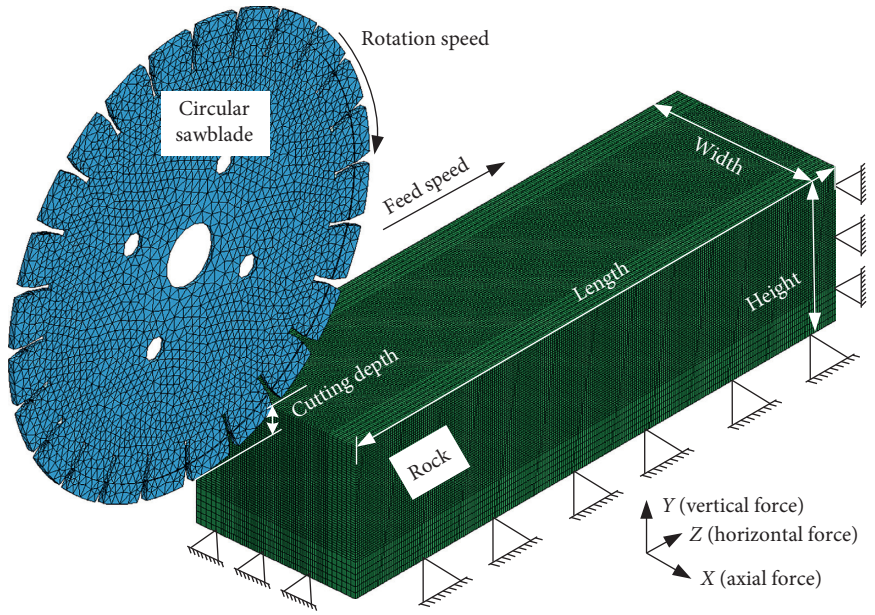

Figure 2: The numerical simulation model of a circular sawblade cutting rock.

$$F_{\text{rate}}(\dot{\varepsilon}) = \begin{cases} \left(\dfrac{\dot{\varepsilon}}{\dot{\varepsilon}_0^c}\right)^{\beta_c}, & p \geq \left(\dfrac{f_c}{3}\right), \\ \dfrac{p + (f_t/3)}{(f_c/3) + (f_t/3)}\left(\dfrac{\dot{\varepsilon}}{\dot{\varepsilon}_0^c}\right)^{\beta_c} + \dfrac{p - (f_c/3)}{-(f_c/3) - (f_t/3)}\left(\dfrac{\dot{\varepsilon}}{\dot{\varepsilon}_0^c}\right)^{\beta_c}, & -\left(\dfrac{f_t}{3}\right) < p < \left(\dfrac{f_c}{3}\right), \\ \left(\dfrac{\dot{\varepsilon}}{\dot{\varepsilon}_0^t}\right)^{\beta_t}, & p \leq -\left(\dfrac{f_t}{3}\right), \end{cases} \tag{7}$$

where f_t is the uniaxial tensile strength; $\dot{\varepsilon}_0^c = 30 \times 10^{-6}\text{s}^{-1}$; $\dot{\varepsilon}_0^t = 3 \times 10^{-6}\text{s}^{-1}$; $\dot{\varepsilon}_0 = 1.0\text{s}^{-1}$; β_c is the compressive strain rate-dependent exponent, $\beta_c = (4/(20 + 3f_c))$; β_t is the tensile strain rate-dependent exponent, $\beta_t = (2/(20 + f_c))$; and f_c is the uniaxial compressive strength.

The equivalent stress of the elastic limit plane of the initial material is obtained by the equivalent stress on the failure plane, with the expression as follows:

$$\sigma_{\text{elastic}}(p, \theta, \dot{\varepsilon}) = f_c \cdot \sigma_{\text{TXC}}^*\left(p_{s,\text{el}}\right) \cdot R_3(\theta) \cdot F_{\text{rate}}(\dot{\varepsilon}) \cdot F_{\text{elastic}} \cdot F_{\text{cap}}, \tag{8}$$

where F_{elastic} is the elastic scaling function, F_{cap} is the cap function, and $p_{s,\text{el}} = (p_s/F_{\text{elastic}})$ is the quasistatic elastic limit pressure.

$$F_{\text{elastic}} = \begin{cases} g_c^*, & p \geq \left(\dfrac{f_{c,\text{el}}}{3}\right) \\ \dfrac{p + \left(f_{t,\text{el}}/3\right)}{\left(f_{c,\text{el}}/3\right) + \left(f_{t,\text{el}}/3\right)} g_c^* + \dfrac{p - \left(f_{c,\text{el}}/3\right)}{-\left(f_{c,\text{el}}/3\right) - \left(f_{t,\text{el}}/3\right)} g_t^*, & -\left(\dfrac{f_{t,el}}{3}\right) < p < \left(\dfrac{f_{c,\text{el}}}{3}\right), \\ g_c^*, & p \leq -\left(\dfrac{f_{t,\text{el}}}{3}\right), \end{cases} \tag{9}$$

where g_c^* is the compression yield surface parameter, $g_c^* = (f_{c,\mathrm{el}}/f_c)$, $f_{c,\mathrm{el}}$ is the uniaxial compression elastic extreme pressure; g_t^* is the tensile yield surface parameter, $g_t^* = (f_{t,\mathrm{el}}/f_c)$; and $f_{t,\mathrm{el}}$ is the uniaxial tensile elastic extreme pressure. The cap function is expressed as

$$F_{\mathrm{cap}} = \begin{cases} 1, & p \le p_u = \left(\dfrac{f_c}{3}\right), \\ \sqrt{1 - \left(\dfrac{p - p_u}{p_0 - p_u}\right)^2}, & p_u < p < p_0, \\ g_c^*, & p \ge p_0 = p_{\mathrm{el}}, \end{cases} \tag{10}$$

where $p_0 = p_{\mathrm{el}}$ is the material porosity break compressive pressure.

Because the RHT constitutive model introduces the linear reinforcement phase equation, it can describe the strain hardening effect of brittle materials such as concrete and rock. In the linear strengthening stage, the yield stress obeys the linear strengthening model. The function expression is

$$\sigma_{\mathrm{Yhard}} = \sigma_{\mathrm{elastic}} + \frac{\varepsilon_{\mathrm{pl}}}{\varepsilon_{\mathrm{pl-presoftening}}} \times \left(\sigma_{\mathrm{fail}} + \sigma_{\mathrm{elastic}}\right), \tag{11}$$

where σ_{fail} is the equivalent stress strength and $\sigma_{\mathrm{elastic}}$ is the equivalent elastic strength.

$$\varepsilon_{\mathrm{pl-presoftening}} = \frac{G_{\mathrm{elastic}}}{G_{\mathrm{elastic}} - G_{\mathrm{plastic}}} \times \frac{\sigma_{\mathrm{fail}} + \sigma_{\mathrm{elastic}}}{3G}, \tag{12}$$

while G is the shear modulus, G_{elastic} is the elastic modulus, and G_{plastic} is the plastic modulus. Combining formulas (11) and (12), the following is obtained:

$$\sigma_{\mathrm{Yhard}} = \sigma_{\mathrm{elastic}} + \frac{3G}{R_G}\varepsilon_p, \tag{13}$$

where ε_p is the plastic strain accumulated in the linear strengthening period and $R_G = (G_{\mathrm{elastic}}/G_{\mathrm{elastic}} - G_{\mathrm{plastic}})$.

At the beginning of the elastic phase and the linear reinforcement of the plastic strain, there is no accumulated damage. Only when the equivalent stress strength exceeds the equivalent stress beyond the failure stress intensity, the material begins to accumulate damage and, then, enters the softening stage of damage. The ratio of the cumulative equivalent plastic strain increase to the ultimate failure equivalent plastic strain is defined as the damage variable D, and the expression is given as

$$0 \le D = \sum \frac{\Delta\varepsilon_p}{\varepsilon_p^{\mathrm{failure}}} \le 1, \tag{14}$$

with

$$\varepsilon_p^{\mathrm{failure}} = D_1 \left(p^* - \mathrm{HTL}^*\right)^{D_2} \ge \varepsilon_p^m. \tag{15}$$

The stress state equation with various different load angles is as follows:

$$R_3(\theta) = \frac{2\left(1 - Q^2\right)\cos\theta + (2Q - 1)\sqrt{4\left(1 - Q^2\right)\cos^2\theta + 5Q^2 4Q}}{4\left(1 - Q^2\right)\cos^2\theta + (2Q - 1)^2}, \tag{16}$$

where Q is the ratio of tension to compression and θ is the load angle.

$$\begin{aligned} \mathrm{HTL}^* &= \frac{\mathrm{HTL}}{f_c}, \\ \mathrm{HTL} &= \frac{f_t}{3} \frac{\left(f_s/\left(f_c R_3^s\right)\right)}{\left(f_s/\left(f_c R_3^s\right)\right) - f_t\left(f_c Q\right)}, \end{aligned} \tag{17}$$

where $\Delta\varepsilon_p$ is the equivalent random strain increase, D_1 and D_2 are the parameters of the material, and ε_p^m is the minimum equivalent plastic strain when the material is destroyed.

The residual stress surface is introduced in the RHT concrete model, and the equivalent stress intensity is σ_{damage}. The expression of σ_{damage} is shown in the following formula:

$$\sigma_{\mathrm{damage}} = (1 - D)\sigma_{\mathrm{failure}} + D\sigma_{\mathrm{residual}}. \tag{18}$$

In the process of circular sawblade cutting rock, the failure modes of rock elements is complex, including compressive failure, tensile failure, and shear failure. Under the action of compressive, tensile, and shear stresses, the damage of rock element appears and increases, while with the rock damage reaching 1, the rock element will fail and be deleted. The rock fragments are difficult to be presented; therefore, the amount of the rock fragments is a positive correlation with rock removal volume. Therefore, the rock fragments are evaluated by rock removal volume.

3.3. Grid Independence Validation. Owing to the grid independence of the simulation model having great influence on the accuracy of simulation results, it is necessary to verify the grid independence. When the relative change rate of cutting force is within the set range scope, the results can be considered reliable and accurate. Finally, the appropriate rock mesh density is selected for the numerical simulation. The relative change rate curve of cutting force under different mesh densities is presented in Figure 3.

When the mesh number reaches 144330, the relative change rate is less than 0.11%, which is within 0.15%. The increase of mesh number has little effect on the relative change rate of the cutting force. Therefore, when the mesh number is more than 144330, the results of numerical simulation can be considered accurate.

3.4. Calibration and Verification. In order to verify the numerical simulation of a circular sawblade cutting rock, in this paper, the experimental results [26] are applied to compare with the numerical simulation with a peripheral speed of 30 m/s, cutting depth of 15 mm, and feed speed of 3 m/min, as shown in Figure 4. The mining values of the vertical and horizontal force at the stable cutting stage are 190.06 N and 137.12 N, respectively, in the experimental

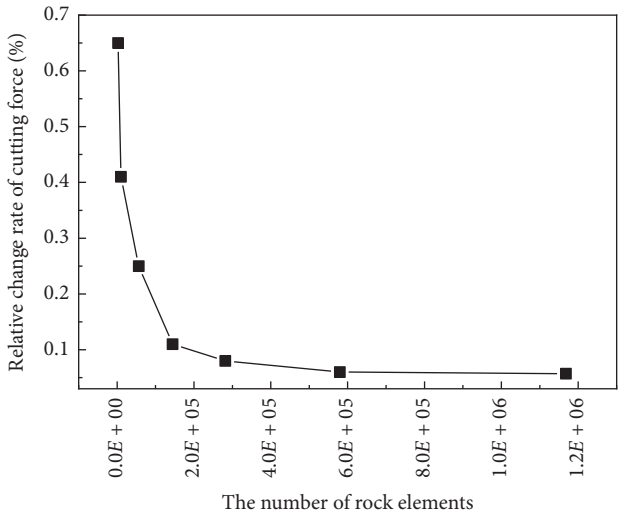

Figure 3: Independence test of the rock mesh density.

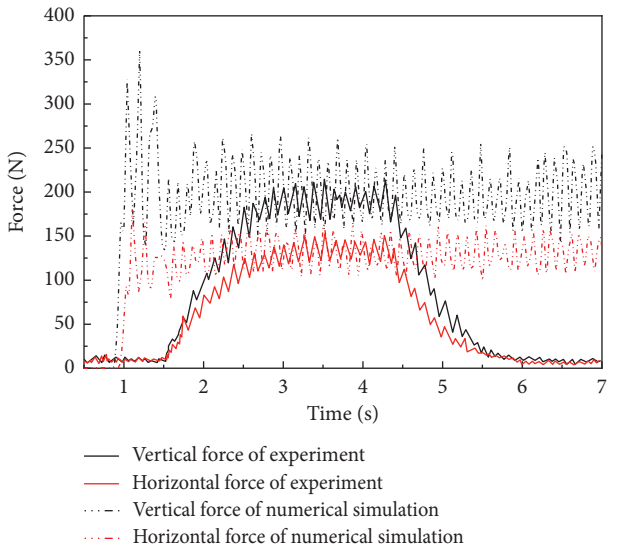

Figure 4: The results of numerical simulation and experiment.

results and 195.26 N and 131.25 N, respectively, in the numerical simulation results. The difference ratio of vertical and horizontal force between experiments and numerical simulation is 2.735% and 4.28%, respectively. The results indicate that the numerical simulation results are in agreement with experimental results, which proves the numerical simulation in this paper is reliable.

4. Results and Discussion

4.1. The Process of a Circular Sawblade Cutting Rock. The circular sawblade cuts rock with constant rotation speed and feed speed, with the feed speed of 0.30 m/min, rotation speed of 2000 r/min, and the cutting depth of 30 mm. It is obvious that the force appears and increases as the circular sawblade contacts the rock. The rock element is damaged with circular sawblade compression and tension. The damage value of some rock elements reaches 1 which is acted by the circular sawblade with continuing cutting. While the damage value of rock element reaches 1, the element would fail and be deleted. The rock damage nephograms in the process of circular sawblade cutting rock are plotted in Figure 5. In the initial stage of rock cutting with a circular sawblade, the deformation and damage of rock appear under compression and tension, as shown in Figure 5(a). With the circular sawblade cutting further, fail elements appear in the first layer elements on the upper surface of the rock and are deleted, as shown in Figure 5(b). While the circular sawblade advances to a certain distance, the rock damage extends outward, and the broken area extends beyond the contacting area. The depth of rock damage increases with the increase in the cutting distance of circular sawblade cutting and reaches a stable depth. Meanwhile, damage ranges also extend and increase downward. When the cutting distance of circular sawblade is large, the damage element on the both sides of saw slot cut by the circular sawblade fail under the interaction of circular sawblade.

The cutting force has a larger peak value when the circular sawblade cuts the rock at the beginning, as shown in Figure 6. The circular sawblade cuts rock at a constant rotation speed and feed speed; at the moment when the circular sawblade contacts the rock which produces a greater impact, the cutting force increases sharply and the peak cutting force is larger than that of stable cutting. It is obvious that the cutting force is closely related to the tangential and normal force, and the wave shape of the normal force curve is similar to the cutting force. The similarity between axial force and cutting force is lower. The values of the normal force and the tangential force are larger than the axial force of a circular sawblade. The fluctuation ranges of the normal force curve and the cutting force are lager; however, the fluctuation of the tangential force curve around the fixed value is relatively stable.

4.2. The Influence of the Rotation Speed Direction of a Circular Sawblade on the Cutting Performance. The circular sawblade cuts rock with the feed speed of 0.30 m/min, rotation speed of 2000 r/min, and the cutting depth of 30 mm. The direction of rotation speed has great effects on the cutting performance. The rock damage nephograms with different rotation speed directions are shown in Figure 7. However, in the numerical simulation results of circular sawblade cut rock with forward cutting, the rock damage area is smaller than that of the reverse cutting. The rock damage ranges of the circular sawblade forward cutting are smaller and more irregular. The broken area is random which is determined by the rock properties. The cutting surface of the circular sawblade is rough, and the quality of rock processing is poor with the circular sawblade reverse cutting, as shown in Figure 7(b). The forward cutting of the circular sawblade can

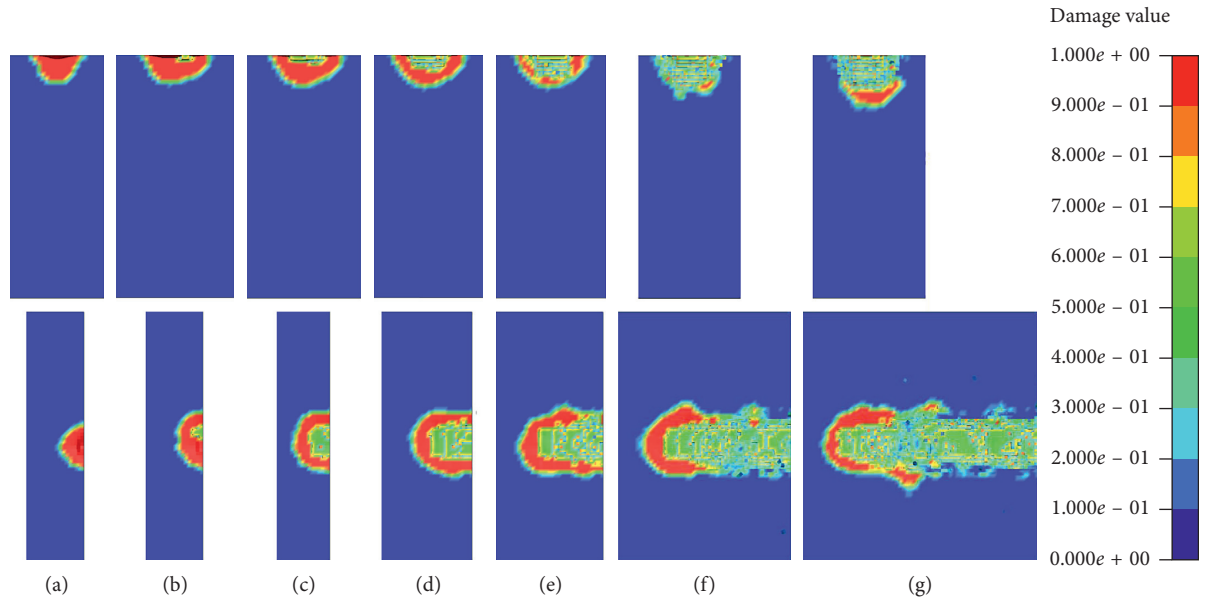

Figure 5: Rock damage nephograms of a circular sawblade cutting rock at various cutting distances: (a) Rock damage nephogram of 7 mm cutting distance; (b) rock damage nephogram of 9 mm cutting distance; (c) rock damage nephogram of 12 mm cutting distance; (d) rock damage nephogram of 21 mm cutting distance; (e) rock damage nephogram of 27 mm cutting distance; (f) rock damage nephogram of 45 mm cutting distance; and (g) rock damage nephogram of 70 mm cutting distance.

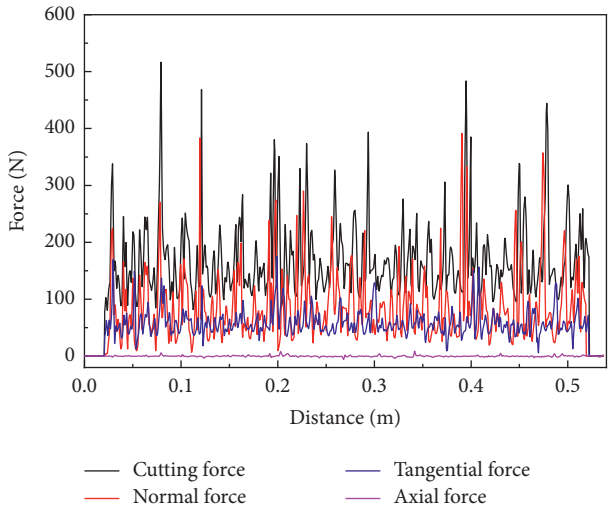

Figure 6: Force curves of rock cutting with a circular sawblade.

achieve perfect quality and the relatively smooth cutting surface. In the left view, the damage area of forward cutting is smaller than that of reverse cutting. Also, the circular sawblade cutting rock with the same cutting parameters, the width and depth of damage area with forward cutting is smaller and more regular than that of the reverse cutting. The damage area of rock is irregular with the reverse cutting, and the quality of rock processing is poor which cannot meet processing requirement. Therefore, the forward cutting is more suitable for rock processing.

The force curves of the circular sawblade cutting rock with the forward cutting and reverse cutting are presented in Figure 8. The cutting force of the forward cutting is smaller than that of the reverse cutting. The force fluctuates steadily with the forward cutting during steady cutting, which is much smaller than that of the reverse cutting. In the process of the circular sawblade cutting rock of the forward cutting, the cutting thickness of each circular grit increases slowly from 0 to the maximum, which makes the amplitude of cutting force smaller. However, when the cutting thickness

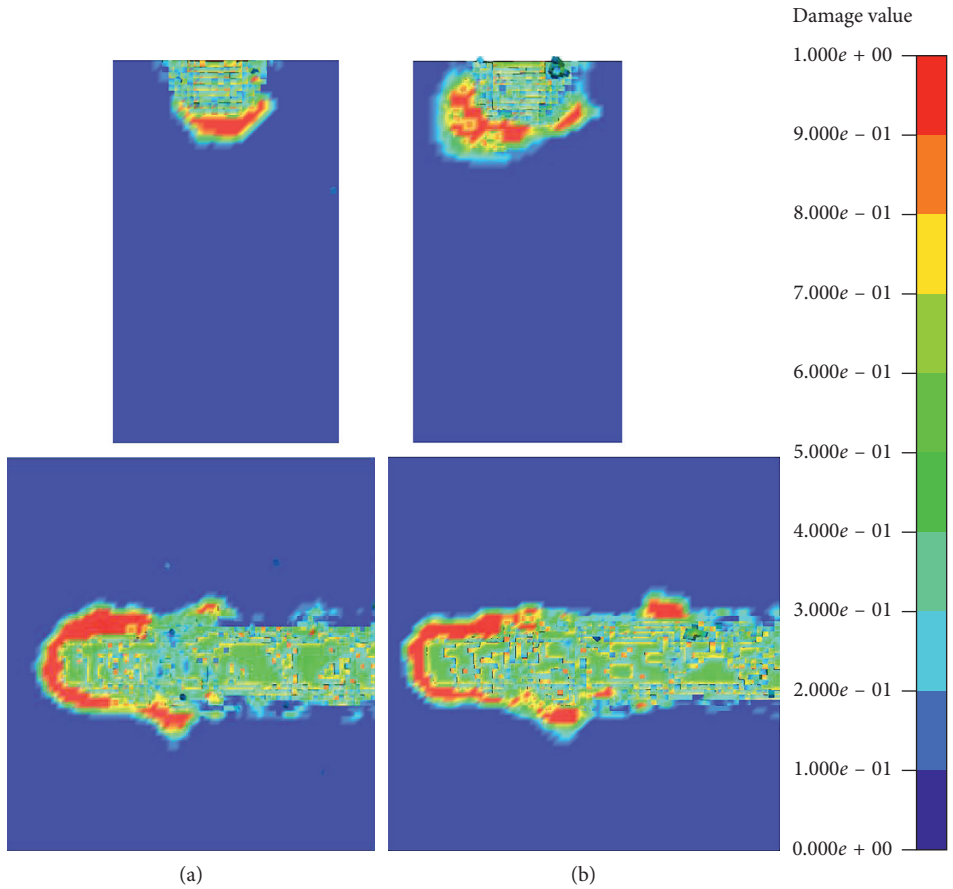

Figure 7: The rock damage nephograms with various cutting models: (a) the rock damage nephogram with forward cutting; (b) the rock damage nephogram with reverse cutting.

of the reverse cutting declines from the maximum value to zero slowly and the compressive strength of rock is large, the fluctuation of cutting force is larger. The wave shape of normal force is basically the same as that of cutting force. Comparing the normal force of the circular sawblade with the forward and reverse cutting, it can be seen that the normal and tangential force amplitude of the forward cutting is smaller than that of the reverse cutting. However, the axial force of forward cutting and the reverse cutting are basically the same.

4.3. The Influence of Cutting Parameters on Cutting Force

4.3.1. The Influence of Feed Speed on Cutting Force. To investigate the influence of feed speed on the cutting force, the circular sawblade cutting rock numerical with the rotation speed of 2000 r/min, the cutting depths of 10, 30, and 50 mm, and the feed speeds of 0.10, 0.15, 0.20, 0.25, and 0.30 m/min are built. The average force curves with various feed speeds are presented in Figure 9. It is obvious that the force increases with the increase of feed speed. While a circular sawblade cuts rock with constant rotation speed, the rock removal volume per circle increases with feed speed increasing, which causes tangential and normal force to increase obviously. The variation trend of the average force curves of cutting force and tangential force is similar. The feed speed increase causes the volume of the rock removal to increase. The difficulty of discharging fragments increasing causes the average axial force increase. However, the growth rate of force with a cutting depth from 30 to 50 mm is larger than that of a cutting depth from 10 to 30 mm. According to Figure 10, the force increases with the cutting depth increasing, and the relationship between the force of circular sawblade and cutting depth is quadratic.

4.3.2. The Influence of Rotation Speed on Cutting Force. The results of the circular sawblade cutting rock with the feed speed of 0.3 m/min, rotation speed of 1000, 1500, 2000, 2500, and 3000 r/min, and cutting depth of 10, 30, and 50 mm are shown in Figure 10. The average force curves of the circular sawblade cutting rock with various rotation speed are presented in Figure 10. It is obvious that the force declines with the rotation speed increasing. The increasing rotation speed reduces the removal volume of rock by a circle of the circular sawblade, which causes the cutting force, normal force, and tangential force to decline, as shown

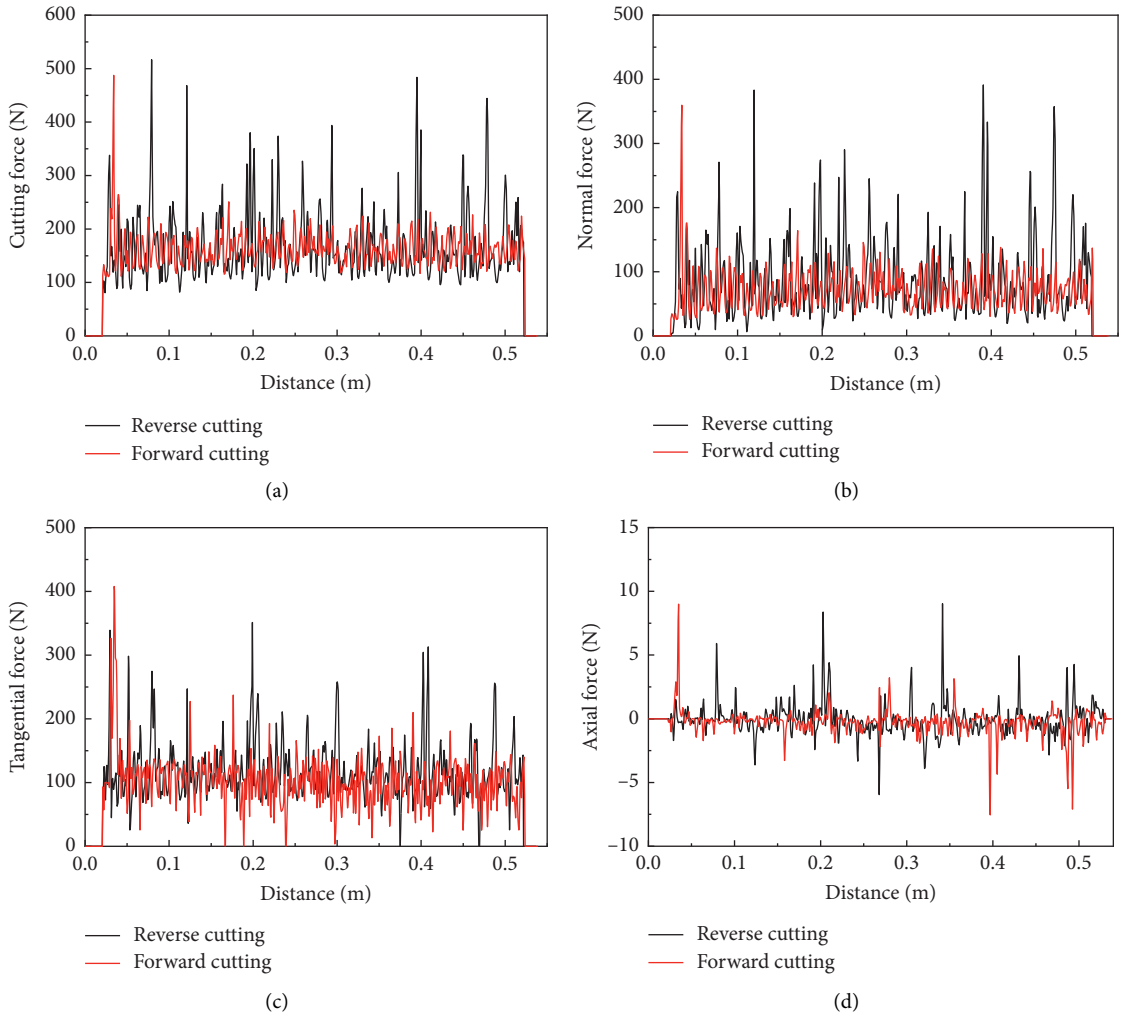

Figure 8: Force curves of the circular sawblade cut rock with forward and reverse cutting: (a) the cutting force of the circular sawblade cutting rock; (b) the normal force of the circular sawblade cutting rock; (c) the tangential force of the circular sawblade cutting rock; and (d) the axial force of the circular sawblade cutting rock.

in Figures 10(a)–10(c). Meanwhile, the removal volume of rock will be decreased by a circle of the circular sawblade cutting rock with the rotation speed increasing, causing the discharge efficiency of rock fragments increasing and the axial force to decrease, as shown in Figure 10(d).

4.3.3. The Influence of Cutting Depth on Cutting Force. Cutting depth is an important cutting parameter which influences cutting force and rock damage. The simulation models with the feed speed of 0.30 m/min, the cutting depths of 10, 20, 30, 40, 50, and 60 mm at the rotation speeds of 1000, 2000, and 3000 r/min are applied to researching influence of cutting depth on cutting force. The cutting force of the circular sawblade cutting rock increases obviously with the increase in cutting depth, as shown in Figure 11. With the increase of cutting depth of the circular sawblade, the rock removal volume by one circle of circular sawblade increasing causes the cutting force, tangential force, and normal force to increase obviously, as presented in Figures 11(a)–11(c). The increasing cutting depth causes the increase of the overlap area between the circular sawblade and rock, which reduces the discharge velocity of rock fragments, and the direct extrusion of rock fragments between circular sawblade and rock increases the axial force of the sawblade, as shown in Figure 11(d).

4.3.4. The Influence of the Distance of Double Circular Sawblades on Cutting Force. The average force curves of double circular sawblades cutting rock with various distances between the double circular sawblades are shown in Figure 12. Also, the distance of the double circular sawblades has a great effect on cutting force, as shown in Figure 12. It is obvious that the cutting force, normal force, and the tangential force increase with the increase in the distance of the circular sawblades, and the cutting force, normal force, and the tangential force of double circular sawblades are smaller

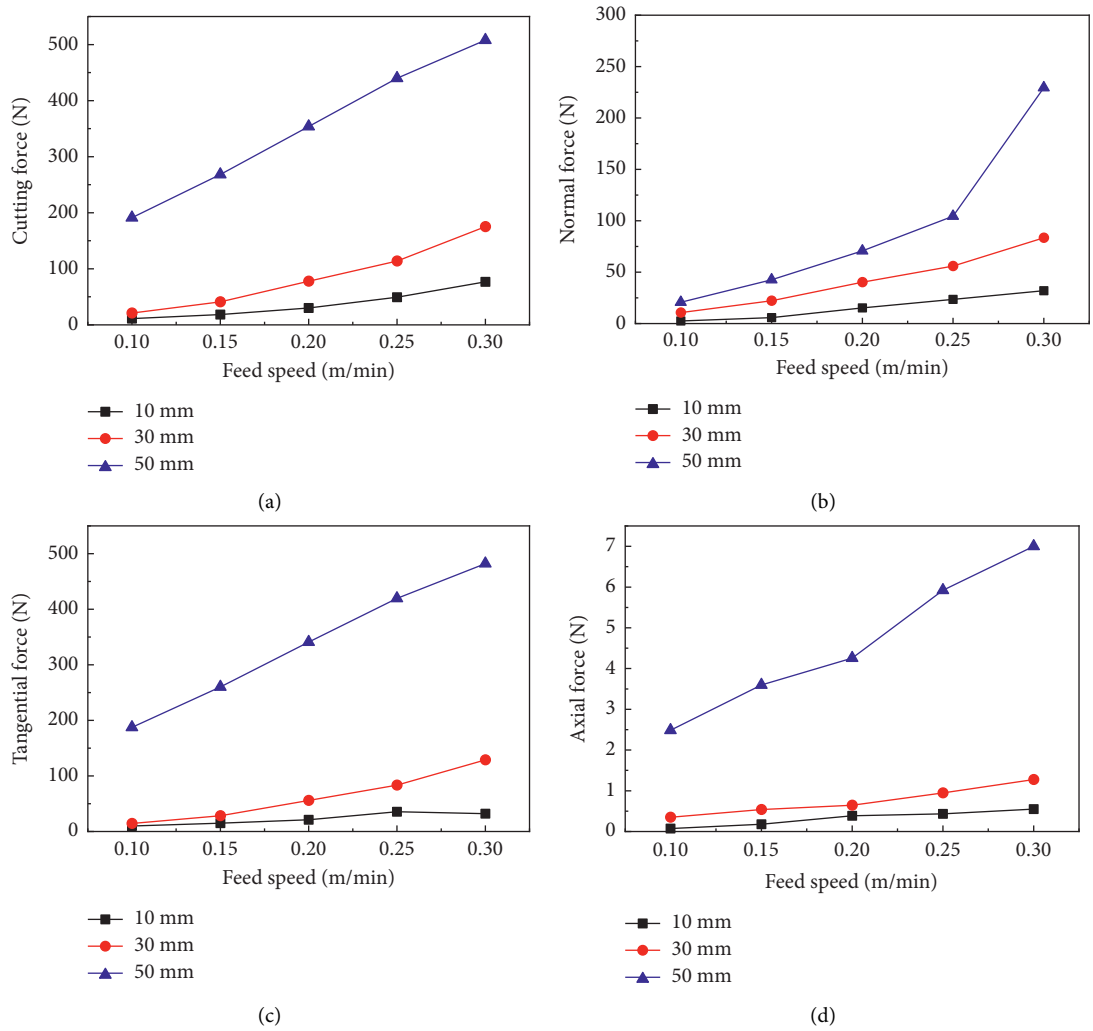

Figure 9: Force curves of the circular sawblade cutting rock with various feed speeds: (a) the cutting force curve of the circular sawblade cutting rock; (b) the normal force curve of the circular sawblade cutting rock; (c) the tangential force curve of the circular sawblade cutting rock; and (d) the axial force curve of the circular sawblade cutting rock.

than that of a single circular sawblade by comparison, as shown in Table 2. Owing to stress superposition, the force of the double circular sawblades is less than that of the single circular sawblade. Therefore, with the distance between the double circular sawblades increasing, the stress superposition effect of the circular sawblades decreases, which causes the cutting force of double circular sawblades to increase. Meanwhile, the average axial force declines with the increase in the distance of double circular sawblades. When the distance is small, the double circular sawblades will affect each other, which causes large axial force.

The results of a single circular sawblade cutting rock are shown in Table 2, with the rotation speed of 2000 r/min, feed speed of 0.30 m/min, and cutting depth of 50 mm, and the double circular sawblades cut rock with the same cutting parameters. The results of single circular sawblade show that the cutting force is 501.51 N, the normal force is 227.85 N, the tangential force is 446.71 N, and the axial force is 6.91 N. However, the results of the double circular sawblade are lower than that of the single sawblade. When the distance between the double circular sawblades reaches 50 mm, the results are close to that of the single circular sawblade. Therefore, it can be concluded that the cutting rock with double circular sawblades can reduce the cutting force.

4.4. The Influence of Cutting Parameters on Rock Damage

4.4.1. The Influence of Feed Speed on Rock Damage. The rock damage area is greatly affected by feed speed, as shown in Figure 13. The damage area in front of the rock with a circular sawblade cutting direction becomes serious with the feed speed increasing. The width of rock damage in front of the cutting direction of the circular sawblade is obviously wider than that behind the circular sawblade. Also, the width of the rock damage area increases with the increase in feed speed. However, the distribution of rock damage is obviously uncertain. Rock removal volume increases with the increase of the feed speed. With constant rotation speed, the higher the

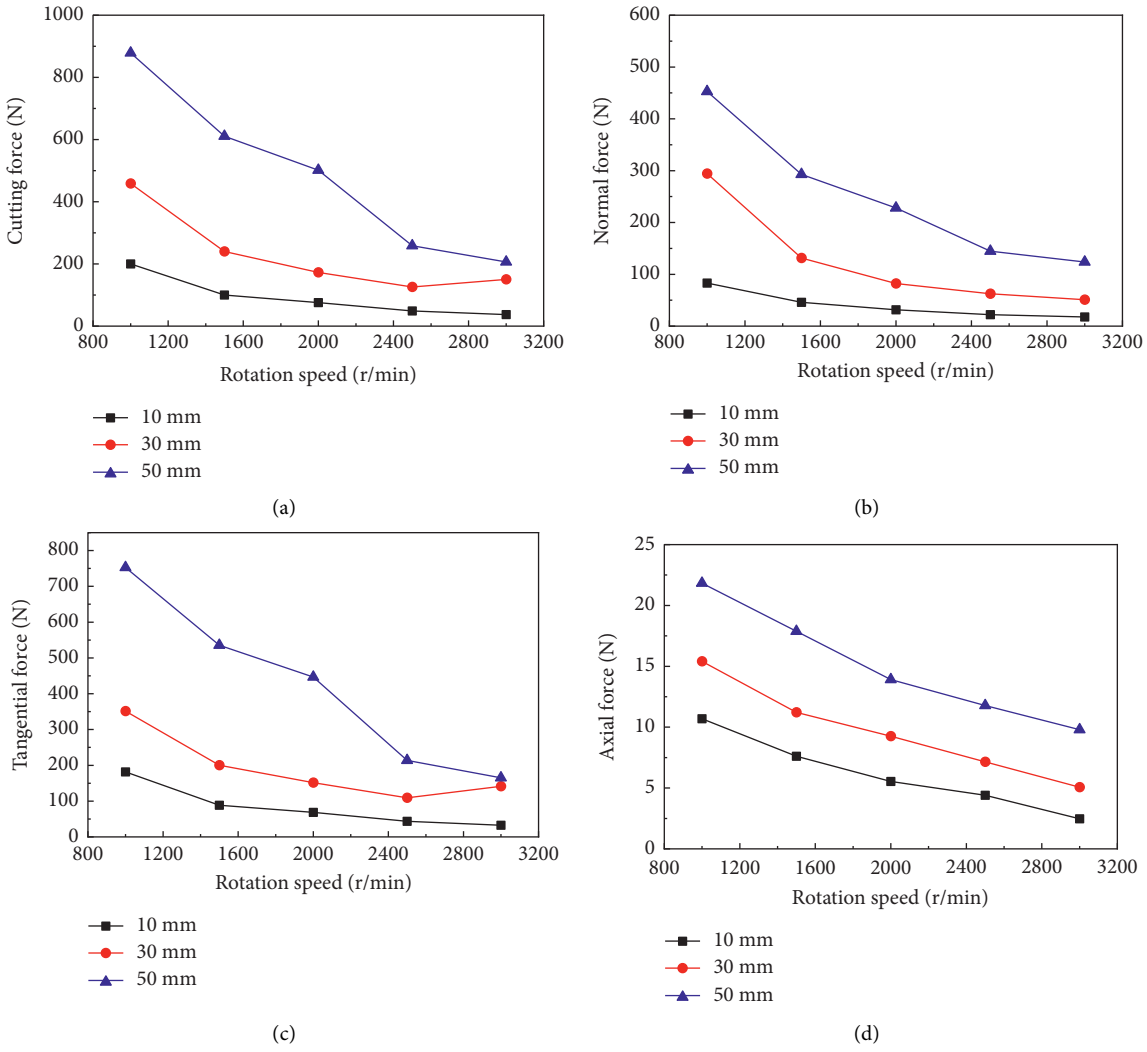

Figure 10: Force curves of the circular sawblade cutting rock with various rotation speeds: (a) the cutting force curve of the circular sawblade cutting rock; (b) the normal force curve of the circular sawblade cutting rock; (c) the tangential force curve of the circular sawblade cutting rock; and (d) the axial force curve of the circular sawblade cutting rock.

feed speed of the circular sawblade, the rougher the sawing seam formed by the circular sawblade cutting rock.

4.4.2. The Influence of Rotation Speed on Rock Damage. In order to research the influence of rotation speed on rock damage, it is defined in the circular sawblade cutting rock in the rotation speeds as 1000, 1500, 2000, 2500, and 3000 r/min, as shown in Figure 14. With the increase in rotation speed, the rock damage area decreases. The width of the rock damage area extends to both sides of the sawing slot decreased at the same cutting depth with the increasing rotation speed. The rock removal volume decreases, and the sawing gap formed by the circular sawblade cutting is smoother. It is obvious that the rock damage area with circular sawblade cutting tends to decrease with the increase of rotation speed. However, the damage of rock in front of the circular sawblade cutting direction is more serious than that behind the circular sawblade.

4.4.3. The Influence of Cutting Depth on Rock Damage. With the increase in cutting depth, the damage of rock increases. As shown in Figure 15, it is obvious that the rock damage is greatly affected by the cutting depth. The rock damage area increases greatly, and the damage area is gradually connected with the increase in cutting depth of the circular sawblade. The rock damage increases with the cutting depth increasing. The width of rock damage increases with the increase in cutting depth, and the deleted amount of rock increases. Meanwhile, the regularity of the rock saw joint is improved. Therefore, increasing the cutting depth of the circular sawblade can improve the processing quality of rock to a certain extent.

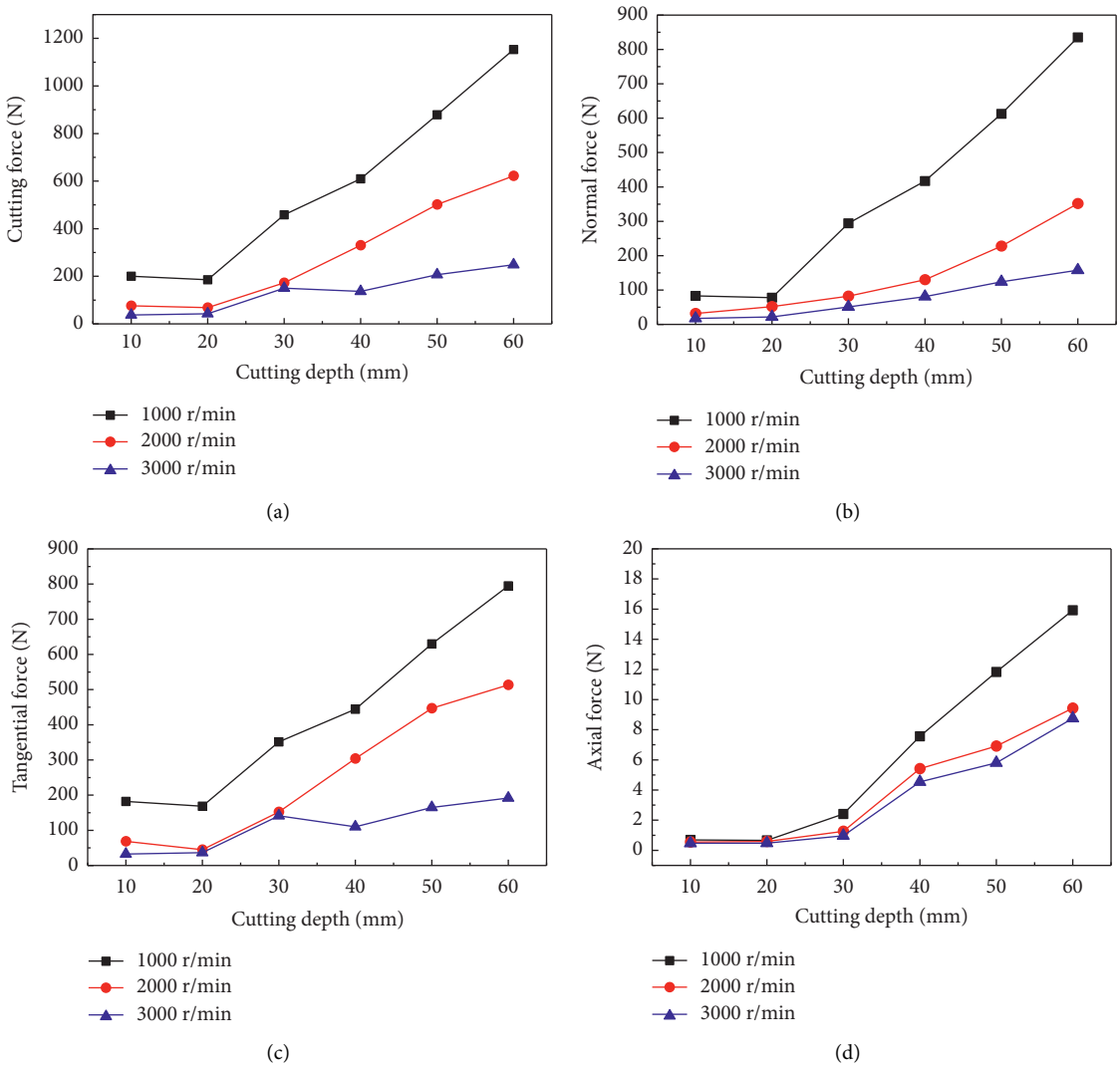

FIGURE 11: Force curves of the circular sawblade cutting rock with various cutting depths: (a) the cutting force curve of the circular sawblade cutting rock; (b) the normal force curve of the circular sawblade cutting rock; (c) the tangential force curve of the circular sawblade cutting rock; and (d) the axial force curve of circular sawblade cutting rock.

4.4.4. The Influence of the Distance between Double Circular Sawblades on Rock Damage. The distance of the double circular sawblades affects the cutting performance. The damage field distributions of the double circular sawblades with various distances between the double circular sawblades are shown in Figure 16. It is obvious that the damage field of rock is superposed by two single damage fields of the circular sawblade. When the distance between the double circular sawblades is small, the overlapping part of damage field of rock between the circular sawblades is large, as shown in Figure 16(a). With the increase of the distance between the circular sawblades, the superimposed damage field changes reduce obviously. When the distance of the double circular sawblades reaches 25 mm, the overlap of the rock damage field disappears, as shown in Figure 16(d). The damage field of rock with circular sawblades cutting affects the area of the rock removal area directly. When the two circular sawblades are close to each other, the overlap of rock damage is larger, which causes the rock slab between the circular sawblades hard to form.

The distance between the double circular sawblades affects the rock damage during circular sawblade cutting rock, as shown in Figure 16. The distance of double circular sawblades affects the formation of rock plate directly. The large stress superposition makes the rock plate between the double circular sawblades difficult to form. When the distance of the double circular sawblades is small, it is difficult to form a relatively complete rock plate between the double circular sawblades. With the increase of the distance between the double circular sawblades, the damage superposition of the double circular sawblades would be weakened, and the rock plate in the middle of the circular sawblades is easier to

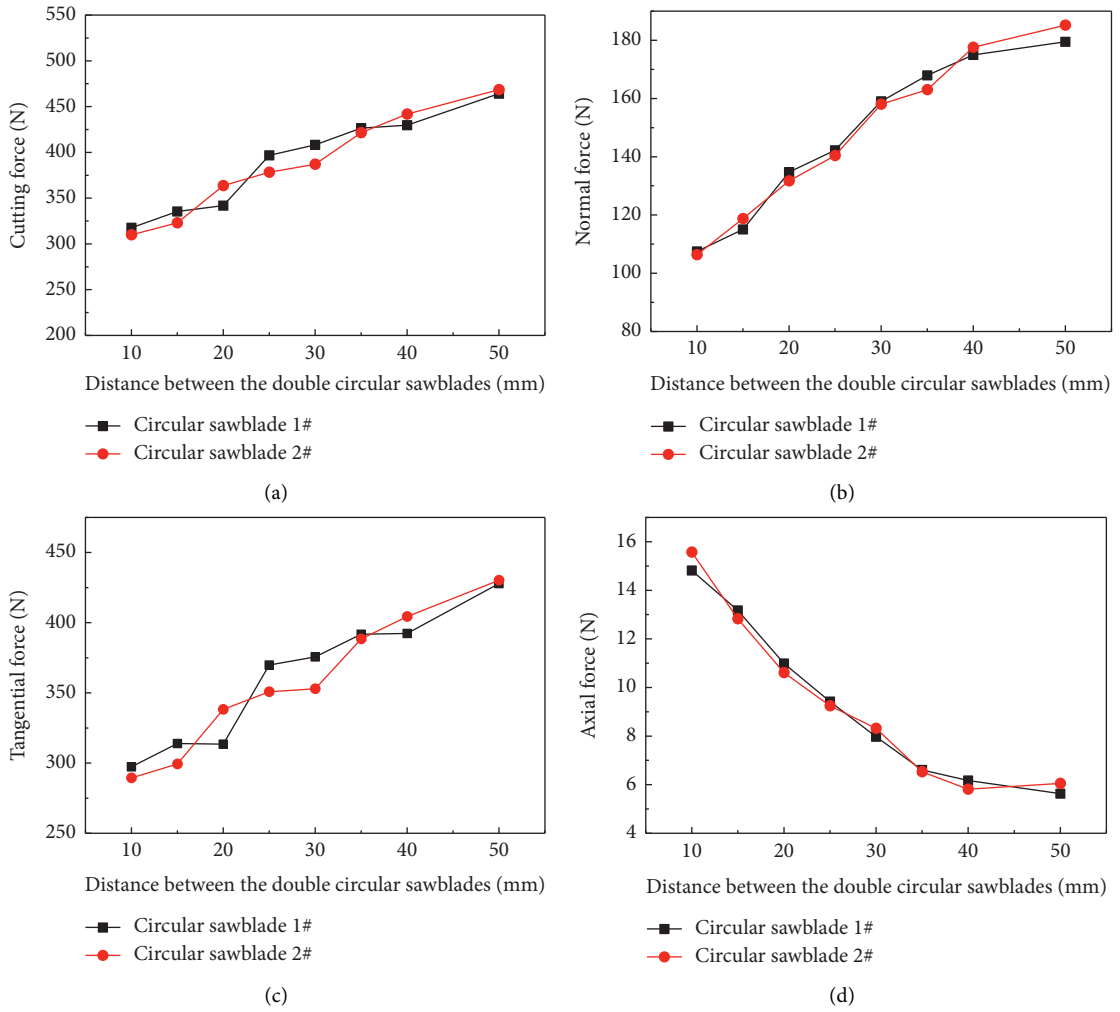

Figure 12: Force curves of the average value of double circular sawblades with various distances: (a) the cutting force curve of double circular sawblades cutting rock; (b) the normal force curve of double circular sawblades cutting rock; (c) the tangential force curve of double circular sawblades cutting rock; and (d) the axial force curve of double circular sawblades cutting rock.

Table 2: The forces of the single and double circular sawblades

Single sawblade		Cutting force (N)		Normal force (N)		Tangential force (N)		Axial force (N)	
		501.51		227.85		446.71		6.91	
	Distance	1#	2#	1#	2#	1#	2#	1#	2#
Double circular sawblade	10	317.6	309.9	107.5	106.3	297.4	289.5	14.8	15.6
	15	335.3	323.0	115.0	118.8	313.9	299.3	13.2	12.8
	20	341.9	363.6	134.7	131.7	313.5	338.2	11.0	10.6
	25	396.7	378.3	142.2	140.4	369.9	350.8	9.4	9.2
	30	408.2	387.1	159.1	158.1	375.6	352.9	8.0	8.3
	35	426.5	421.5	168.0	163.0	391.8	388.5	6.6	6.5
	40	429.7	441.8	175.0	177.6	392.3	404.3	6.2	5.8
	50	464.1	468.6	179.5	185.2	427.9	430.3	5.6	6.1

form. The amount of rock removal volume of the double circular sawblade cutting declines with the increase of the distance between the double circular sawblades.

4.5. The Influence of the Cutting Parameter on Specific Cutting Energy. The specific energy consumption is an important index to evaluate the cutting performance of a circular

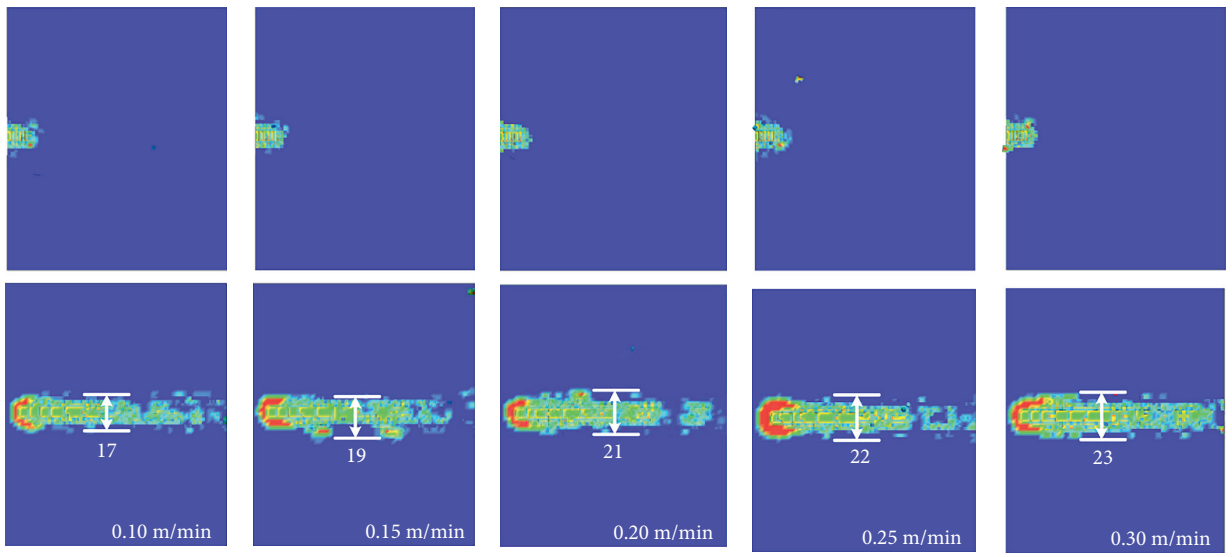

Figure 13: Rock damage nephogram with various feed speeds: (a) feed speed of 0.10 m/min; (b) feed speed of 0.15 m/min; (c) feed speed of 0.20 m/min; (d) feed speed of 0.25 m/min; and (e) feed speed of 0.30 m/min.

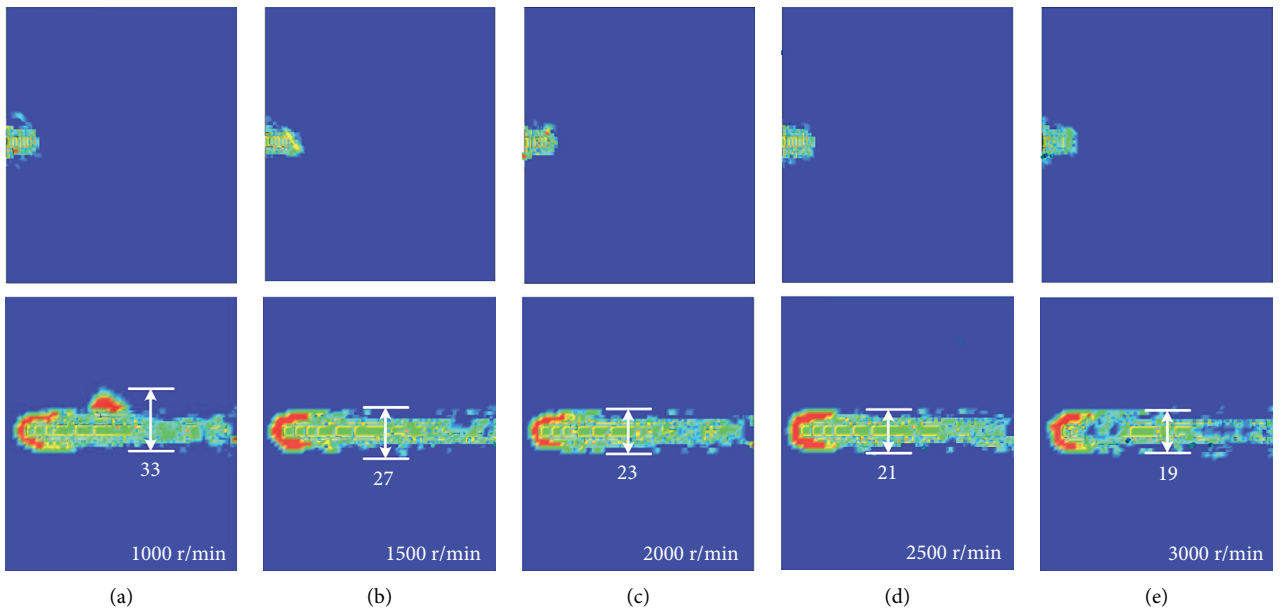

Figure 14: Rock damage nephogram with various rotation speeds: (a) rotation speed of 1000 r/min; (b) rotation speed of 1500 r/min; (c) rotation speed of 2000 r/min; (d) rotation speed of 2500 r/min; and (e) rotation speed of 3000 r/min.

sawblade. The cutting energy of a circular sawblade cutting rock is defined as the product of tangential force and relative moving distance of the circular sawblade, and the specific cutting energy is defined as the ratio of the cutting energy consumption to rock removal volume.

$$\mathrm{SE} = \frac{F_t \cdot s}{V}, \tag{19}$$

where SE is the specific cutting energy, s is the relative moving distance of the circular sawblade and rock, and V is the rock removal volume.

The specific cutting energy of the circular sawblade cutting rock with various cutting parameters is shown in Figures 17 and 18. The relationship between the specific energy consumption and the cutting depth of the circular sawblade is presented in Figure 17. The specific cutting

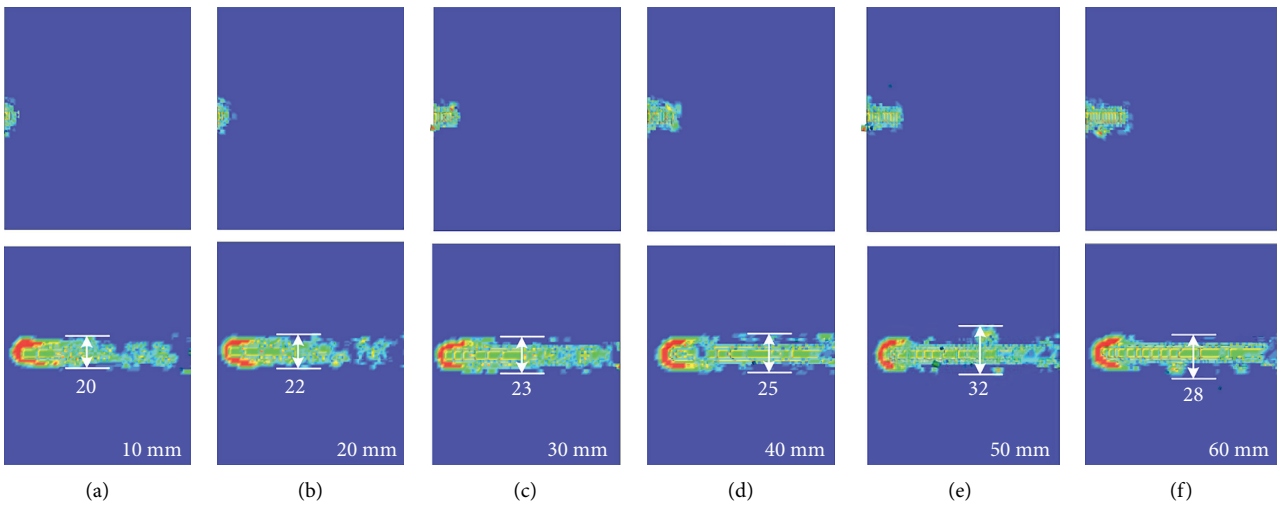

Figure 15: Rock damage nephogram with various cutting depths: (a) cutting depth of 10 mm; (b) cutting depth of 20 mm; (c) cutting depth of 30 mm; (d) cutting depth of 40 mm; (e) cutting depth of 50 mm; and (f) cutting depth of 60 mm.

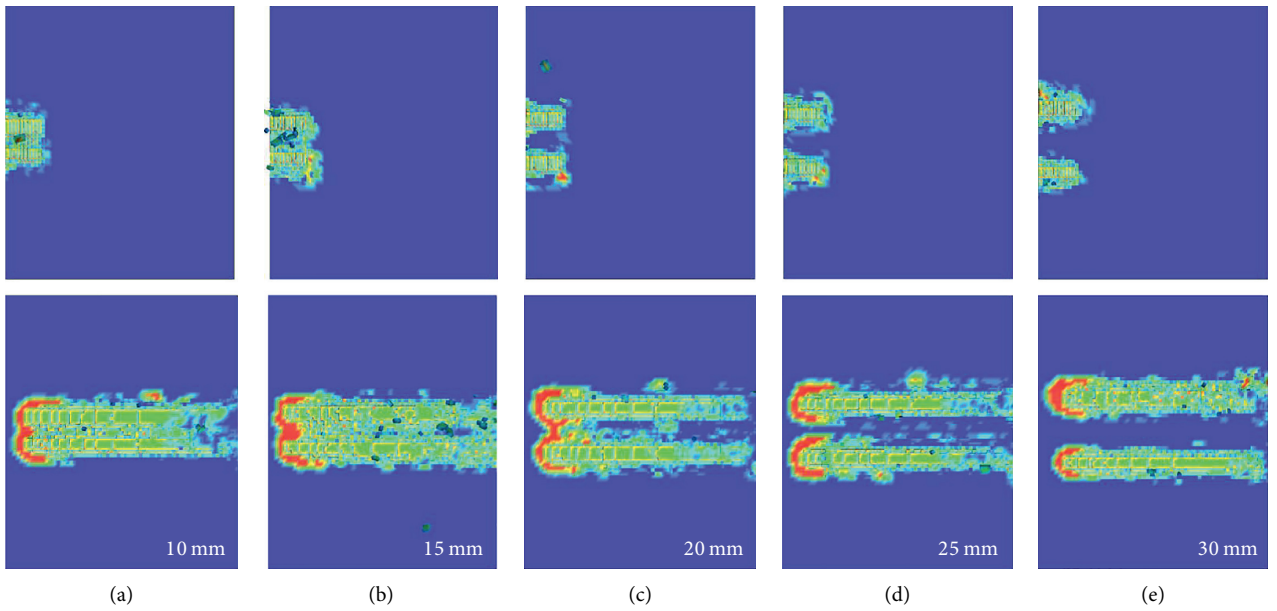

Figure 16: Rock damage nephogram with various distances between double circular sawblades: (a) distance between doubled circular sawblades of 10 mm; (b) distance between doubled circular sawblades of 15 mm; (c) distance between doubled circular sawblades of 20 mm; (d) distance between doubled circular sawblades of 25 mm; and (e) distance between doubled circular sawblades of 30 mm.

energy consumption declines with cutting depth increasing. The relationship between the specific cutting energy and distance between the double circular sawblades is shown in Figure 18. The specific cutting energy of the double circular sawblades increases with the increase in distance between double circular sawblades, the increasing trend slows down, and the specific cutting energy tends to be stable. The specific cutting energy consumption of the double circular sawblades is less than that of the single circular sawblade. The expressions of the fitting relationship between the specific cutting energy consumption and cutting depth and the distance between the double circular sawblades are shown in Table 3. The specific cutting energy consumption decreases, and the specific cutting energy consumption increases with the increase in circular sawblade spacing, to a certain extent.

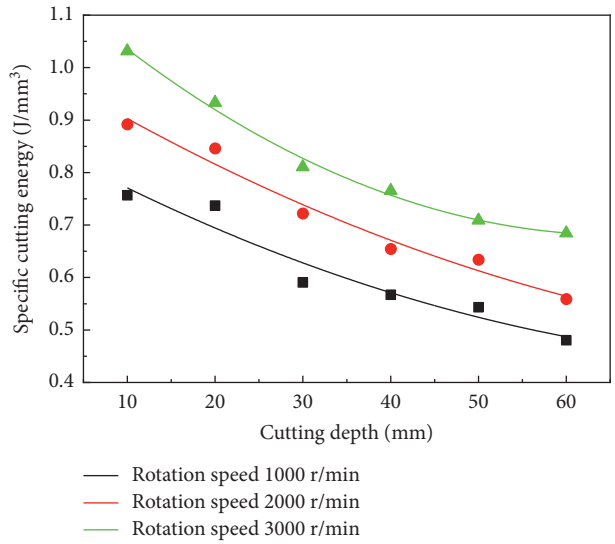

Figure 17: The relationship of the specific cutting energy and cutting depth.

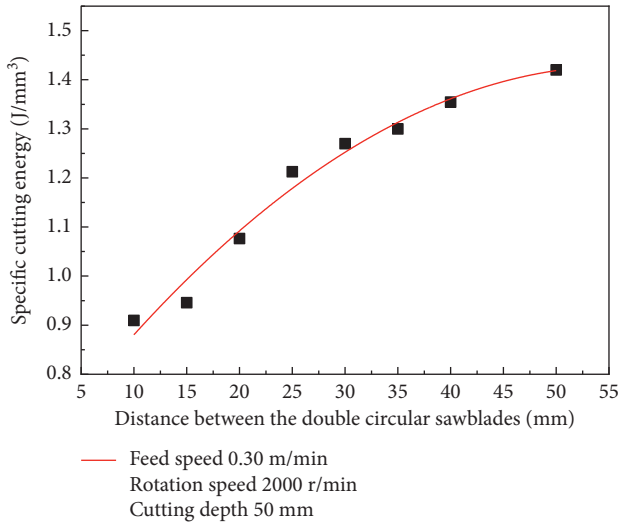

Figure 18: Relationship between the specific cutting energy consumption and the distance between the circular sawblades.

Table 3: The regression results to predict the specific cutting energy.

Variables	Cutting parameters	Regression equation	Correlation coefficient	F value	P value
SE-CD	RS = 1000 r/min	$y = 0.00246x^2 - 0.04554x + 0.42847$	0.89530	602.2663	$1.2383E-4$
SE-CD	RS = 2000 r/min	$y = 0.0024x^2$-$0.05062x + 0.49967$	0.95913	1556.879	$2.8962E-5$
SE-CD	RS = 3000 r/min	$y = 0.00567x^2 - 0.07476x + 0.58671$	0.99008	7631.371	$2.7548E-6$
SE-DD	FS = 0.3 m/min RS = 2000 r/min	$y = -0.000128x^2 + 0.01443x + 0.30879$	0.95239	3850.399	$1.0724E-8$

SE = specific energy, CD = cutting depth, DD = distance between the double circular sawblades

5. Conclusions

The process of the circular sawblade cutting rock is studied in this paper. The influence of cutting parameters and the direction of the circular sawblade on the cutting performance are explored.

(1) Cutting parameters have a great effect on the cutting performance. The cutting force increases with the feed speed, and cutting depth increasing and declines with the increase of rotation speed. The increasing distance of double sawblades causes the cutting force to increase and, then, maintain stable.

(2) The damage and rock removal volume of the rock are influenced by the cutting parameters of the circular sawblade. When the damage of rock reaches 1, the rock elements will fail and be deleted. Therefore, the rock removal volume is closely related to rock damage. The forward cutting and reverse cutting have different influences on rock damage and cutting force. The fluctuation of the forward cutting force curve is much smaller than that of the reverse cutting force curve.

(3) The cutting parameters of the circular sawblade influence the specific cutting energy. The specific cutting energy decreases with the increase in cutting depth, and the specific cutting energy increases with the increase of the distance between double circular sawblades.

The results of the researches could be used to guide rock processing.

Data Availability

The data used to support the findings of this study are included within the article.

Conflicts of Interest

There are no conflicts of interest regarding the publishing of this paper.

Acknowledgments

This work was supported by the projects of the National Natural Science Fund of China (Grant nos. 51674155 and 51974170) and the Natural Science Foundation of Shandong Province (Grant no. ZR2019BEE069).

References

[1] H. Zhang, J. Zhang, and S. Wang, "Comparison of wear performance of diamond tools in frame sawing with different trajectories," *International Journal of Refractory Metals and Hard Materials*, vol. 78, pp. 178–185, 2019.

[2] G. Yan, Y. Wu, He Wang, D. Zhao, and F. Lu, "Research on mathematical model and cutting characteristics in machining of natural marble by diamond coated tool," *Mechanics*, vol. 25, no. 2, pp. 165–171, 2019.

[3] T.-M. Oh, G.-W. Joo, Y. Cha, and G.-C. Cho, "Effect of garnet characteristics on abrasive waterjet cutting of hard granite rock," *Advances in Civil Engineering*, vol. 2019, Article ID 5732649, 12 pages, 2019.

[4] F. Wang, S. Liu, and K. Ji, "Numerical study on abrasive machining of rock using FDEM method," *Simulation Modelling Practice and Theory*, vol. 104, p. 102145, 2020.

[5] P. Dong, H. Bo, J. Zhang, and H. Zhang, "Investigation and improvement of wear nonuniformity of diamond tools in sawing granite," *International Journal of Refractory Metals and Hard Materials*, vol. 83, p. 104961, 2019.

[6] H. D. Jerro, S. S. Pang, C. Yang, and R. A. Mirshams, *Kinetic Analysis of Chipping Materials Using Superabrasive Diamond Tools*, American Society of Mechanical Engineers (ASME), New York; NY, USA, 1995.

[7] S. Turchetta, L. Sorrentino, and C. Bellini, "A method to optimize the diamond wire cutting process," *Diamond and Related Materials*, vol. 71, pp. 90–97, 2017.

[8] Y. Zhong, E. Kuru, H. Zhang, J. Kuang, and J. She, "Effect of fracturing fluid/shale rock interaction on the rock physical and mechanical properties, the proppant embedment depth and the fracture conductivity," *Rock Mechanics and Rock Engineering*, vol. 52, no. 4, pp. 1011–1022, 2019.

[9] I. Karakurt, G. Aydin, and K. Aydiner, "Experimental and statistical analysis of cutting force acting on diamond sawblade in sawing of granitic rocks," *Proceedings of the Institution of Mechanical Engineers, Part B: Journal of Engineering Manufacture*, vol. 227, no. 2, pp. 286–300, 2013.

[10] I. S. Buyuksagis and R. M. Goktan, "Investigation of marble machining performance using an instrumented block-cutter," *Journal of Materials Processing Technology*, vol. 169, no. 2, pp. 258–262, 2005.

[11] A. Ersoy and U. Atici, "Performance characteristics of circular diamond saws in cutting different types of rocks," *Diamond and Related Materials*, vol. 13, no. 1, pp. 22–37, 2004.

[12] M. Fener, S. Kahraman, and M. O. Ozder, "Performance prediction of circular diamond saws from mechanical rock properties in cutting carbonate rocks," *Rock Mechanics and Rock Engineering*, vol. 40, no. 5, pp. 505–517, 2007.

[13] D. Tumac, "Predicting the performance of large diameter circular saws based on Schmidt hammer and other properties for some Turkish carbonate rocks," *International Journal of Rock Mechanics and Mining Sciences*, vol. 75, pp. 159–168, 2015.

[14] F. Wang, S. Liu, Z. Guo, and L. Cao, "Analysis of cutting forces and chip formation in milling of marble," *The International Journal of Advanced Manufacturing Technology*, vol. 108, no. 9-10, pp. 2907–2916, 2020.

[15] S. Kahraman, H. Altun, B. S. Tezekici, and M. Fener, "Sawability prediction of carbonate rocks from shear strength parameters using artificial neural networks," *International Journal of Rock Mechanics and Mining Sciences*, vol. 43, no. 1, pp. 157–164, 2006.

[16] D. Tumac and A. Shaterpour-Mamaghani, "Estimating the sawability of large diameter circular saws based on classification of natural stone types according to the geological origin," *International Journal of Rock Mechanics and Mining Sciences*, vol. 101, pp. 18–32, 2018.

[17] D. Tumac, "Artificial neural network application to predict the sawability performance of large diameter circular saws," *Measurement*, vol. 80, pp. 12–20, 2016.

[18] X. Wie, C. Wang, and Z. Zhou, "Study on the fuzzy ranking of granite sawability," *Journal of Materials Processing Technology*, vol. 139, no. 1–3, pp. 277–280, 2003.

[19] S. Kahraman, M. Fener, and O. Gunaydin, "Predicting the sawability of carbonate rocks using multiple curvilinear regression analysis," *International Journal of Rock Mechanics and Mining Sciences*, vol. 41, no. 7, pp. 1123–1131, 2004.

[20] S. Kahraman and O. Gunaydin, "Indentation hardness test to estimate the sawability of carbonate rocks," *Bulletin of Engineering Geology and the Environment*, vol. 67, no. 4, pp. 507–511, 2008.

[21] M. Yurdakul and H. Akdas, "Prediction of specific cutting energy for large diameter circular saws during natural stone cutting," *International Journal of Rock Mechanics and Mining Sciences*, vol. 53, pp. 38–44, 2012.

[22] A. Güney, "Performance prediction of large-diameter circular saws based on surface hardness tests for Mugla (Turkey) marbles," *Rock Mechanics and Rock Engineering*, vol. 44, no. 3, pp. 357–366, 2011.

[23] M. C. Shaw, *Principles of Abrasive Processing*, Oxford Science, Oxford, UK, 1996.
[24] X. Xu, Y. Li, and S. Malkin, "Forces and energy in circular sawing and grinding of granite," *Journal of Manufacturing Science & Engineering*, vol. 123, no. 1, pp. 305–312, 2001.
[25] Z. Lu, Q. Zeng, Z. Meng, Z. Wang, and G. Gao, "Numerical simulation on cutting and fracturing of rock plate with one side fixed and three sides free," *Advances in Materials Science and Engineering*, vol. 2020, Article ID 8652637, 14 pages, 2020.
[26] X. Xu, Y. Li, and Y. Yu, "Force ratio in the circular sawing of granites with a diamond segmented blade," *Journal of Materials Processing Technology*, vol. 139, no. 1–3, pp. 281–285, 2003.